New insight in the Hawaiian plume swell dynamics from scaling laws

Jeroen van Hunen and Shijie Zhong
Univ. Colorado, Dept. Physics, Boulder, Colorado, USA

Received 29 April 2003; revised 2 June 2003; accepted 10 June 2003; published 1 August 2003.

[1] The formation and shape variation of the Hawaiian plume swell is re-examined numerically. Scaling laws for the plume buoyancy flux and swell width and height help gaining new insight in relationships between swell formation and relevant model parameters, like plume temperature and size, and mantle rheology. A scaling law for the plume buoyancy $F = A\eta_0^{-1.2}R_p^{3.5}\Delta T_p^{2.2}\exp(1.3 \times 10^{-8}E\Delta T_p)$, with background mantle viscosity η_0, plume radius R_p, plume excess temperature ΔT_p, and activation energy E fits numerical flux measurements within 8%. Scaling laws for the swell width and height have similar forms, and their multiplication resembles the buoyancy flux scaling law within 10%. These scaling laws suggest that the background mantle viscosity plays a significant role, and that the increased Hawaiian plume intensity ~25 Ma ago is due to a plume excess temperature increase of 50%. *INDEX TERMS:* 8120 Tectonophysics: Dynamics of lithosphere and mantle—general; 8121 Tectonophysics: Dynamics, convection currents and mantle plumes; 9355 Information Related to Geographic Region: Pacific Ocean. **Citation:** van Hunen, J., and S. Zhong, New insight in the Hawaiian plume swell dynamics from scaling laws, *Geophys. Res. Lett.*, *30*(15), 1785, doi:10.1029/2003GL017646, 2003.

1. Introduction

[2] The linear age-progressive characteristics of the Hawaiian volcanic chain are believed to originate from interaction between an ascending thermal plume and the overriding Pacific plate [*Morgan*, 1971]. Another important feature associated with plume-plate interaction is a surrounding bathymetric swell with ~1 km in height and ~1000 km in width (Figures 1a and 1b) [*Davies*, 1988; *Olson*, 1990]. Such swell topography is of particular interest in the studies of mantle dynamics, because it constrains plume buoyancy flux that may be related to the cooling rate of the core [*Davies*, 1988; *Sleep*, 1990].

[3] Significant progress has been made in understanding the dynamics of plume-plate interaction through analytic models of lubrication theory and 3-D numerical modeling. *Olson* [1990] proposed that buoyant plume material spreading below a moving lithosphere gives isostatic swell topography that can be predicted from a lubrication theory. *Ribe and Christensen* [1994, 1999] supported Olson's theory with 3-D numerical models for a range of plume buoyancy fluxes and plate velocities. *Phipps Morgan et al.* [1995] emphasized the role of the buoyant depleted mantle associated with hotspot volcanism in producing the swell. *Zhong and Watts* [2002] found that swell topography from plume-plate interaction may explain the uplift history of some Hawaiian islands.

[4] However, these studies explored only a limited model parameter space for plume-plate interaction, and are difficult to be used to understand the time-dependent nature of the Hawaiian swell topography and plume buoyancy flux as documented by *Davies* [1992] and *Wessel* [1993] (Figure 1b). Here, we develop scaling laws for plume buoyancy flux, swell width and height, using 3-D numerical modeling of plume-plate interaction for a wide range of plume and mantle viscosity parameters. We apply the scaling laws to understand the nature of the time dependence of the Hawaiian swell.

2. Numerical Model Setup

[5] We use a parallel Cartesian 3-D version of the numerical finite element model Citcom [*Moresi and Gurnis*, 1996; *Zhong et al.*, 2000] to simulate the interaction of the Hawaiian plume with the overlying Pacific lithosphere (Figure 1a). The model is similar to the one used in [*Zhong and Watts*, 2002], which, in turn, is based on the model presented by *Ribe and Christensen* [1994]. The model is 400 km deep, 3200 km long (i.e. in the plate motion direction) and 1600 km wide. It is symmetric about $y = 0$, and calculations are only done for $y > 0$ (Figure 1a). An oceanic plate, being 0°C at the surface, moves in the positive x-direction at v_p = 8.6 cm/yr, which corresponds to the absolute Pacific plate motion. A plume is created by assigning a hot circular region at the bottom, centered at $(x,y) = (0,0)$ with a temperature anomaly $\Delta T(r) = \Delta T_p \exp(-r^2/R_p^2)$ with ΔT_p and R_p fixed maximum excess temperature and radius of the plume stem, and r the distance from the plume center. Our model aims to study the local area around the plume at high-resolution, and only a larger-scale model could be dynamically more self-consistent without prescribing the parameters ΔT_p and R_p. We use flow-through boundary conditions. The bottom has fixed T = 1350°C + ΔT, and zero normal stress which permits vertical flow. Inflow at $x = -800$ km is specified with a temperature that corresponds to a 80-Ma old oceanic mantle and horizontal velocity consistent with v_p, zero horizontal motion at the bottom, and the viscosity structure [*Ribe and Christensen*, 1994]. A zero normal conductive heat flux boundary condition is applied at the outflow boundary, and to assure mass conservation, the outflow velocity is equal to the inflow.

[6] A linear viscous Arrhenius rheology for diffusion creep was assumed, using

$$\eta = \eta_0 \exp\left[\frac{E}{R}\left(\frac{1}{T} - \frac{1}{T_m}\right)\right], \quad (1)$$

0094-8276/03/2003GL017646$05.00

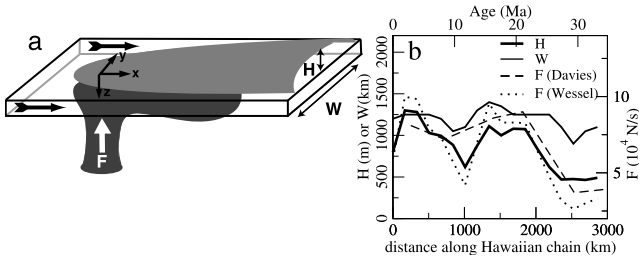

Figure 1. (a) Schematic plot of the plume-lithosphere interaction near Hawaii. (b) Data plot for H (thick line) and W (thin line) taken from [*Wessel*, 1993], and the buoyancy flux F from [*Davies*, 1992] (dashed) and [*Wessel*, 1993] (dotted, see text). All curves show a significant increase towards Hawaii around 25 Ma.

with η_0 the viscosity for $T = T_m = 1350°C$, and E the activation energy. Using the Boussinesq approximations and an infinite Prandtl number fluid, we solve for the conservation of mass, momentum, and temperature. Details are given in [*Zhong and Watts*, 2002].

3. Results

[7] The numerical model is used to determine the relationship between model parameters and model observations, including plume buoyancy, swell height and swell width. As pointed out by *Olson* [1990] and *Ribe and Christensen* [1994], the shape of the plume swell is largely controlled by the plume buoyancy flux, mantle rheology, and velocity of the lithospheric plate. We further elaborate the dependence of these model observations on η_0, E, ΔT_p, and R_p with a large number of calculations, in which we varied each of these model parameters over a plausible range. We vary η_0 from 5×10^{19} to 4×10^{20} Pa s, E from 120 to 240 kJ/mol, ΔT_p from 300 to 400 K, and R_p from 45 to 120 km. In total, 72 model calculations are used in this study, of which about half were conducted in [*Zhong and Watts*, 2002]. These calculations produce a buoyancy flux that varies over more than an order of magnitude, and a swell width and height variation of over half an order of magnitude.

3.1. Buoyancy Flux

[8] First we develop a scaling law that relates the plume buoyancy flux F to the model parameters. Before examining numerical results, we consider a simple 1-D analytical pipe flow model that provides us guidance to develop the scaling law. Let R_p be the radius of a hot plume pipe with constant excess temperature $\Delta T = \Delta T_p$. The buoyancy force per vertical segment dz of a cylinder with radius $r \le R_p$ is $\pi r^2 \delta\rho g dz$. The shear force at the cylinder side is $2\pi r \eta \frac{du}{dr} dz$. Equating those relations gives an expression for $\frac{du}{dr}$. Ignoring deformation for $r > R_p$, where due to lower temperature the viscosity is much larger, integration over r gives $u(r)$, and $F = \int_0^{R_p} 2\pi r' u(r') \delta\rho dr' \propto \frac{R_p^4 \Delta T_p^2}{\eta}$. A first order Taylor expansion, $\eta \approx \eta_0 \exp(-E\Delta T_p/(RT_m^2))$ leads to

$$F \propto \eta_0^{-1} R_p^4 \Delta T_p^2 \exp\left(\frac{E}{R} \frac{\Delta T_p}{T_m^2}\right). \quad (2)$$

[9] In the numerical models, $F = \int_{\Omega_b} v_z \delta\rho d\Omega_b$ in which v_z is the upward vertical velocity. F is monitored through the entire bottom boundary Ω_b. Time-dependent model calculations are performed until a steady state buoyancy flux is obtained. Results show linear relationships in log-log plots of F [kg/s] against η_0 [Pa s], ΔT_p [°C], and R_p [km], and exponential dependence of F on E [J/mol], thus consistent with the simple 1-D analytical model of Equation 2. We therefore fit our numerical results of F with a scaling law:

$$F_0 = A\eta_0^{a_F} R_p^{b_F} \Delta T_p^{c_F} \exp\left(d_F F \Delta T_p\right). \quad (3)$$

Best fitting prefactor and exponents are given in Table 1. The exponents correspond reasonably well with the theoretical ones from Equation 2. Deviations are likely due to 1) the proximity of the lithosphere in the 3-D model, whereas the theory uses a simple 1-D approach, and 2) the radially varying plume stem temperature. The fit of numerical results to Equation 3 is shown in Figure 2a, for which the standard deviation of the relative misfit is 7.9%. The fit for the theoretical Equation 2 is much worse with a 105% misfit. Fixing a_F, b_F, and c_F to their theoretical values, and allowing only d_F to vary also gives a significant error of 34%, while fixing a combination of three other exponents makes the fit even worse. Overall, the theory provides a good basis for the scaling law, but fine-tuning of a_F to d_F is necessary to describe the 3-D character.

3.2. Width and Height of the Plume Swell

[10] Next we derive scaling laws for the width $W(x)$ and height $H(x)$ of the plume swell. Because the plume buoyancy flux is proportional to the product of plume width, plume height, and plate velocity [*Davies*, 1988; *Sleep*, 1990; *Ribe and Christensen*, 1994], we assume that a similar scaling law basis as in Equation 3 applies. We will show a posteriori that this assumption is correct. A steady state model buoyancy flux is quickly reached, but a steady state plume swell shape takes longer time integration. We selected 46 calculations with steady state swell shape. Width and height of each swell are calculated from the topography δh relative to the situation without a plume [*Ribe and Christensen*, 1994].

[11] Since convective instabilities within the swell [*Moore et al.*, 1998] do not occur for the chosen set of model parameters, we can define the plume W and H from δh which makes direct comparison with Hawaiian swell observations straightforward. $H(x)$ [m] is defined as δh at the symmetry axis $y = 0$, and $W(x)$ [km] as the y-coordinate to where δh is reduced to 100 m. $W(x)$ ranges from 250 to 1500 km (Figure 3a), while the maximum height H_{max} varies between 750 and 2500 m (Figure 3b). With the same method as for the buoyancy flux scaling law in Equation 3, we determine exponents a, b, c, and d to describe the

Table 1. Prefactor and Exponents for Scaling Laws of the Form $f = A\eta_0^a R_p^b \Delta T_p^c \exp(dE\Delta T_p)$ with f being the Buoyancy Flux F, Swell Width W, or Swell Height H

	A*	a#	b	c	d
flux F (kg/s)	1.6×10^{15}	−1.2	3.5	2.2	1.3×10^{-8}
width W (km)	2.9×10^{13}	−0.8	1.8	0.7	1.0×10^{-8}
height H (m)	1.2×10^{6}	−0.5	1.7	1.7	1.6×10^{-9}

*For W and H, the prefactor A is calculated for maximum height and corresponding width.

#For W and H, the exponents a, b, c, and d are averages over $x > 250$ km.

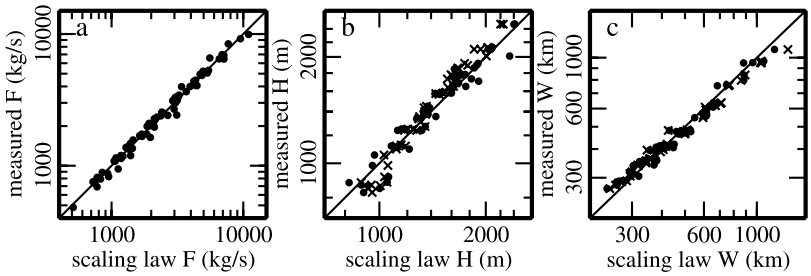

Figure 2. Fit of numerical values (vertical axis) to the scaling law prediction (horizontal axis) for (a) the plume buoyancy flux F, (b) the maximum swell height H_{max} for our scaling (circles) and the *Ribe and Christensen* [1999]-scaling (crosses), and (c) the corresponding width W.

dependence on η_0, R_p, ΔT_p, and the exponential term, respectively, for both W and H as a function of x for $-50 \le x \le 1750$ km (Figure 4). Although these exponents fluctuate substantially near the plume center, where the plume still feeds the swell, they are nearly constant for $x >$ 250 km. The exponents $\bar{a}$, $\bar{b}$, $\bar{c}$, and $\bar{d}$ for both W and H are averages for $a(x)$, $b(x)$, $c(x)$, and $d(x)$ from Figure 4 for $x >$ 250 km. These averages form the basis for scaling laws for H and W at maximum height H_{max} and corresponding width:

$$H_0 = A_H \eta_0^{\bar{a}_H} R_p^{\bar{b}_H} \Delta T_p^{\bar{c}_H} \exp\left(\bar{d}_H E \Delta T_p\right). \quad (4)$$

$$W_0 = A_W \eta_0^{\bar{a}_W} R_p^{\bar{b}_W} \Delta T_p^{\bar{c}_W} \exp\left(\bar{d}_W E \Delta T_p\right). \quad (5)$$

Values for these average exponents, A_H, and A_W are given in Table 1. The fit of the scaling laws is illustrated in Figures 2b and 2c for H_{max} and corresponding width W with a relative misfit standard deviation of 7.4% and 7.2%, respectively. The fit for other x is approximately the same. The relation $F \sim W \times H$ is confirmed by our scaling laws: multiplication of W_0 and H_0 agrees with F_0 within 10% for a, b, c, and d (see Table 1).

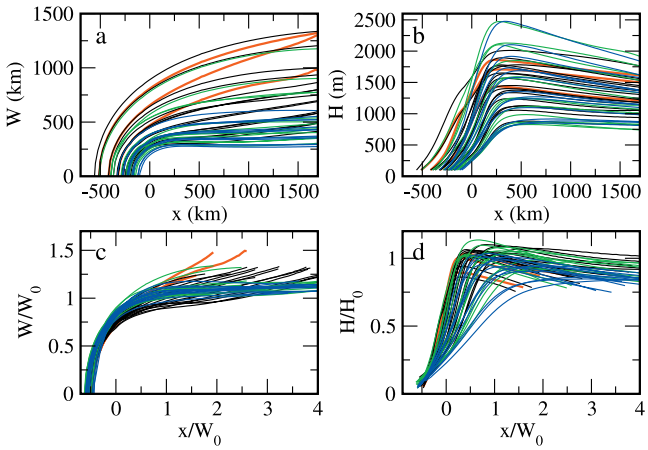

Figure 3. Swell dimensions: (a) $W(x)$, (b) $H(x)$, (c) scaled width $W' = W/W_0$, and (d) scaled height $H' = H/H_0$ as a function of x/W_0. Each curve corresponds to one 3-D model calculation. Red, black, green, and blue curves refer to $\eta_0 = 5 \times 10^{19}$, 10^{20}, 2×10^{20}, and 4×10^{20} Pa s, respectively.

[12] We further scaled each of the curves in Figures 3a and 3b with their scaling law values from Equations 5 and 4. Results for W/W_0 and H/H_0 as a function of x/W_0 are shown in Figures 3c and 3d. To first order, the scaled curves cluster on top of one another, because much of the dependence of W and H on η_0, R_p, ΔT_p, and E is removed by the scaling. The remaining spreading indicates what is not included in the scaling law. Obviously, the major portion of this remainder is due to the x-dependence of the curves: W and H change with the distance from the plume center, and this information is still included after scaling. Interestingly, this x-dependence is not the same for all curves. In the scaled W-curves, a pattern can be recognized: smaller η_0 tends to cause continued lateral spreading of the swell downstream (Figure 3c).

3.3. Hawaiian Buoyancy Flux Variations

[13] Hawaiian swell observations indicate that both width and height have increased substantially at 25 Ma. Height data from *Wessel* [1993] and width data from Figure 6 in [*Wessel*, 1993] are shown in Figure 1b, together with F-data from *Davies* [1992] and from Wessel's width and height values, using a formulation by *Sleep* [1990]. The difference between these two independent calculations of the plume buoyancy flux can be regarded as the uncertainty in this estimate. At around 25 Ma, F-estimates show an increase of a factor 2.5 to 4. At the same time, H approximately doubles, while W increases much less.

[14] Our scaling laws for F, W and H may help to distinguish which model parameter may have changed and caused these observed variations. The scaling law exponents suggest that a growth of R_p would increase H and W by the same fraction, and increase F twice as much (see Table 1), inconsistent with the observations. Following the same reasoning, a decrease in η_0 would affect the width

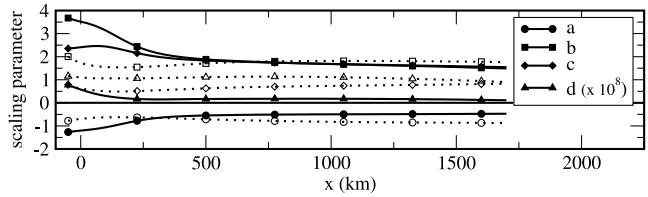

Figure 4. Scaling exponents $a(x)$, $b(x)$, $c(x)$, and $d(x)$ for height (solid lines) and width (dashed lines). Averages over $x >$ 250 km are used to construct H_0 and W_0 in Equations 4 and 5.

more than the height, which is also not observed, and agrees with a sudden change in η_0 being physically unlikely, because η_0 relates to the global temperature in the ambient mantle. Increasing ΔT_p, on the contrary, would increase the swell height much more than the width, which is in agreement with the observations. This suggests that at around 25 Ma, the plume may have become hotter, rather than just more voluminous, and a 50% ΔT_p-increase fits the observations best.

4. Discussion and Conclusions

[15] We studied the dynamics of the interaction between a buoyant plume and a moving oceanic lithosphere. Based on 72 calculations with different plume and mantle viscosity parameters, we developed scaling laws for the plume buoyancy flux and the swell width and height. We find that multiplication of the scaling laws for the swell width and height corresponds well to the scaling law for the plume buoyancy flux. Those scaling laws suggest that the width and the height of the swell are not in the same way sensitive to changes in plume temperature, viscosity, or plume radius, and that the rapid increase of the Hawaiian plume intensity at around 25 Ma was most likely caused by a 50% increase in the plume excess temperature.

[16] Although ΔT_p and R_p may not be entirely independent, and an increase in the former could result in a change in the latter, we believe that such change in the plume radius is secondary. Furthermore, this application of our scaling laws implicitly assumes that the swell response to changes in the plume characteristics is instantaneous. Time-dependent modeling tests show that this response time is at most 5 Ma, and therefore quick enough for the above analysis.

[17] Our results suggest that the background viscosity plays a role in the swell shape. This is different from the lubrication theory [*Olson*, 1990] that suggests that the plume viscosity controls the plume dynamics. *Ribe and Christensen* [1994] showed that for this theory, far-downstream $W \propto (x - x_p)^m$, with $m = 1/5$, which fits their numerical results for a (pressure-dependent) rheology with $\eta_0 = 10^{21}$ Pa s and $E = 200$ kJ/mol. We fit the downstream parts of the scaled curves from Figure 3c to this powerlaw relation, using a linear least-squares method. We find that m varies between approximately 0 to 0.4, depending on η_0 and E. This range envelopes the $m = 1/5$ by *Ribe and Christensen* [1994].

[18] Based on the same lubrication theory, *Ribe and Christensen* [1999] find that height and width scale as $\delta\rho(Q/\sigma)^{1/4}G(\Pi_b)/(\rho_0 - \rho_w)$ and $C_W Q^{3/4}\ \sigma^{1/4}/(UG(\Pi_b))$, respectively, with $Q = F/\delta\rho$, $\sigma = g\delta\rho/(48\eta_p)$, U the plate velocity, η_p the minimum plume viscosity, and G empirical function of the plume buoyancy parameter $\Pi_b = Q\sigma/U^2$. Due to model differences (rheology, bottom boundary conditions, and definitions of H and W), and different rheological parameter range, our results require a variation in G of more than a factor 3, and do not fit $G = 1.26 \tanh(1.01 \times 10^{-2}\Pi_b + 0.687)$ proposed in [*Ribe and Christensen*, 1999]. Instead we find $G(\Pi_b) = 0.1 \ln(98\Pi_b + 1)$, and $C_W = 1$ to fit our data with a relative misfit of 7.8% and 7.1% for H and W, respectively. These misfits are comparable to our scaling law, and are added to Figures 2b and 2c for H_{max} and corresponding W. The function G might reflect a missing background viscosity term in the scaling. This would correspond to previous work by *Feighner and Richards* [1995] who suggested that the plume viscosity alone does not properly describe the spreading of the plume material. Furthermore, scaling of the data with the method in [*Ribe and Christensen*, 1999] and properly fitting G also shows similar fanning related to the background viscosity η_0, as in Figures 3c and 3d. Our results and comparison with [*Ribe and Christensen*, 1999] seem to suggest that lubrication theory describes the swell spreading well to first order, but a more accurate incorporation of the rheology is needed to improve the fit of scaling laws to the data, and that the background viscosity plays a significant role in it.

[19] **Acknowledgments.** We want to thank Neil Ribe and Norm Sleep for constructive reviews, and Tony Lowry and Garrett Ito for fruitful discussions. This study is funded by David and Lucile Packard Foundation and NSF under Grant number EAR 0134939.

References

Davies, G. F., Ocean bathymetry and mantle convection 1. large-scale flow and hotspots, *J. Geophys. Res.*, *93*, 10,467–10,480, 1988.

Davies, G. F., Temporal variation of the Hawaiian plume flux, *Earth Plan. Sci. Let.*, *113*, 277–286, 1992.

Feighner, M. A., and M. A. Richards, The fluid dynamics of plume-ridge and plume-plate interactions: An experimental investigation, *Earth Plan. Sci. Let.*, *129*, 171–182, 1995.

Moore, W. B., G. Schubert, and P. Tackley, Three-dimensional simulations of plume-lithosphere interaction at the Hawaiian swell, *Science*, *279*, 1008–1011, 1998.

Moresi, L., and M. Gurnis, Constraints on the lateral strength of slabs from three-dimensional dynamic flow models, *Earth Plan. Sci. Let.*, *138*, 15–28, 1996.

Morgan, W. J., Convection plumes in the lower mantle, *Nature*, *230*, 42, 1971.

Olson, P., Hot spots, swells and mantle plumes, in *Magma transport and storage*, pp. 33–51, John Wiley, New York, 1990.

Phipps Morgan, J., W. J. Morgan, and E. Price, Hotspot melting generates both hotspot volcanism and a hotspot swell?, *J. Geophys. Res.*, *100*, 8045–8062, 1995.

Ribe, N. M., and U. R. Christensen, Three-dimensional modelling of plume-lithosphere interaction, *J. Geophys. Res.*, *99*, 669–682, 1994.

Ribe, N. M., and U. R. Christensen, The dynamical origin of Hawaiian volcanism, *Earth Plan. Sci. Let.*, *171*, 517–531, 1999.

Sleep, N. H., Hotspots and mantle plumes: Some phenomenology, *J. Geophys. Res.*, *95*, 6715–6736, 1990.

Wessel, P., Observational constraints on models of the Hawaiian hot spot swell, *J. Geophys. Res.*, *98*, 16,095–16,104, 1993.

Zhong, S., and A. B. Watts, Constraints on the dynamics of mantle plumes from uplift of the Hawaiian islands, *Earth Plan. Sci. Let.*, *203*, 105–116, 2002.

Zhong, S., M. T. Zuber, L. Moresi, and M. Gurnis, Role of temperature-dependent viscosity and surface plates in spherical shell models of mantle convection, *J. Geophys. Res.*, *105*, 11,063–11,082, 2000.

J. van Hunen and S. Zhong, Department of Physics, University of Colorado at Boulder, Campus Box 390, Boulder, CO 80309-0390, USA. (hunen@colorado.edu)